

γ -ray spectroscopy of proton neutron-hole nucleus ^{208}Bi from deep inelastic heavy ion reactions

B. Fornal and R. Broda

*Niewodniczański Institute of Nuclear Physics, PL-31342 Cracow, Poland
and Chemistry Department, Purdue University, West Lafayette, Indiana 47907*

K. H. Maier

Oak Ridge National Laboratory, Oak Ridge, Tennessee 37831

P. J. Daly, P. Bhattacharyya, and Z. W. Grabowski

Chemistry and Physics Departments, Purdue University, West Lafayette, Indiana 47907

W. Królas, T. Pawłat, and J. Wrzesiński

Niewodniczański Institute of Nuclear Physics, PL-31342 Cracow, Poland

M. P. Carpenter, R. V. F. Janssens, F. G. Kondev, T. Lauritsen, D. Seweryniak, and I. Wiedenhöver

Physics Division, Argonne National Laboratory, Argonne, Illinois 60439

S. Lunardi, C. A. Ur, and G. Viesti

Dipartimento di Fisica dell'Università' and INFN, Sezione di Padova, I-35131 Padova, Italy

M. Cinausero and N. Marginean

INFN, Laboratori Nazionali di Legnaro, I-35020 Legnaro, Italy

M. Rejmund

Dapnia/SPhN, CEA Saclay, F-91191 Gif sur Yvette Cedex, France

(Received 30 September 2002; published 25 March 2003)

γ rays in the $\pi\nu^{-1}$ nucleus ^{208}Bi have been studied at the Gammasphere using deep-inelastic reactions induced by a 305-MeV ^{48}Ca beam on a thick ^{208}Pb target. Previously unknown yrast γ -ray cascades above the 10^{-} millisecond isomer in ^{208}Bi were identified in cross coincidence with known γ rays from complementary potassium products. Yrast and near-yrast levels up to 5.6 MeV in ^{208}Bi have been located, and they are interpreted in light of earlier charged particle spectroscopy results, and with the help of shell model calculations.

DOI: 10.1103/PhysRevC.67.034318

PACS number(s): 21.60.Cs, 23.20.Lv, 27.80.+w, 25.70.Lm

I. INTRODUCTION

The ^{208}Bi nucleus is a one-proton-particle, one-neutron-hole system with respect to the doubly magic ^{208}Pb core. Its level structure at low excitation energies arises from $1p$ - $1h$ couplings involving $1h_{9/2}$, $2f_{7/2}$, and $1i_{13/2}$ proton particles, and $3p_{1/2}$, $2f_{5/2}$, $3p_{3/2}$, and $1i_{13/2}$ neutron holes. The ^{208}Bi ground state has the configuration $(\pi h_{9/2}\nu p_{1/2}^{-1})5^{+}$, with the $J^{\pi}=4^{+}$ member of the same multiplet lying 63 keV higher. All the other $1p$ - $1h$ states involving the $h_{9/2}$ proton have been identified in the 0.5–2.9 MeV energy range by Crawley *et al.* [1], who performed high energy resolution $^{209}\text{Bi}(p,d)$ transfer reaction measurements. The highest spin states identified were the $J^{\pi}=10^{-}$ and 11^{-} states of $\pi h_{9/2}\nu i_{13/2}^{-1}$ character; from earlier γ -ray studies, this 10^{-} state is a known 2.58-ms isomer at 1571 keV [2], and the (p,d) measurements located the 11^{-} state 858 ± 3 keV above the 10^{-} isomer.

At about 3 MeV of excitation energy one may expect states arising from the coupling of $f_{7/2}$ proton particle and $i_{13/2}^{-1}$ neutron hole. However, since the $\pi f_{7/2}$ single-particle

orbital lies 900 keV above the $\pi h_{9/2}$, there is little chance that these configurations could be close enough to the yrast line to be seen in the present γ study.

Yrast $1p$ - $1h$ states involving the $i_{13/2}$ proton particle and $i_{13/2}^{-1}$ neutron hole should occur at somewhat higher excitation energies. All that is known about these states comes from $^{208}\text{Pb}(p,n)$ charge exchange reaction studies of Anderson *et al.* [3], who located in ^{208}Bi at about 3.4 MeV a strong candidate for the $(\pi i_{13/2}\nu i_{13/2}^{-1})13^{+}$ fully stretched state, although the angular distribution does not rule out 11^{+} for all or part of the observed peak.

Above 3.5 MeV, the ^{208}Bi yrast level structure will increase in complexity as excitations of neutrons across the $N=126$ shell gap become possible. A special class of states are those arising from $2p$ - $2h$ configurations involving combinations of one-proton particle and one-neutron particle with two neutron holes coupled to 0^{+} (as in the ^{206}Pb ground state). Three ^{208}Bi states of this type with $I^{\pi}=11^{+}$, 12^{+} , and 14^{-} and the aligned configurations $\pi i_{13/2}\nu g_{9/2}\times^{206}\text{Pb}(0^{+})$, $\pi h_{9/2}\nu j_{15/2}\times^{206}\text{Pb}(0^{+})$, and $\pi i_{13/2}\nu j_{15/2}\times^{206}\text{Pb}(0^{+})$, respectively, have been located in the 3.5–5.0 MeV range by

Daehnick and Spisak [4,5] using the $^{206}\text{Pb}(\alpha, d)$ reaction.

The ^{208}Bi nucleus cannot be reached in heavy ion fusion-evaporation reactions with stable beams, and its yrast level structure above the 10^- isomer has thus far not been explored by γ -ray spectroscopy.

Since nearly a decade, deep-inelastic reactions have been used successfully for structure investigations of neutron-rich nuclei [6]. In such deep-inelastic collisions, the production yield is spread over many nuclei, but the resolving power of the large detector arrays has proven sufficient to extract detailed information from coincidence datasets with large statistics, even for weak reaction channels.

In the present work, high-spin states in ^{208}Bi (and many other nuclei) were populated by deep-inelastic reactions occurring during $^{48}\text{Ca}+^{208}\text{Pb}$ heavy ion collisions, and extensive γ -ray coincidence measurements performed using the Gammasphere multidetector array established additional yrast and near-yrast states in ^{208}Bi extending to about 5.6 MeV. Interpretation of the ^{208}Bi level structures above the 10^- isomer will be presented, highlighting the significant overlap between the present results and those from charged particle reaction spectroscopy. Energy comparisons with shell model calculations will also be discussed, and the role of octupole excitations will be considered.

II. EXPERIMENTAL PROCEDURE AND RESULTS

The experiment was performed at the Argonne National Laboratory using Gammasphere array and a 305-MeV ^{48}Ca beam from the ATLAS accelerator. A 50 mg/cm^2 ^{208}Pb target was placed in the center of the detector array, which consisted of 101 Compton-suppressed Ge detectors. γ -Ray coincidence data were collected with a trigger requiring three or more Compton-suppressed γ rays to be in coincidence within a 200 ns time range. Each event stored energy and timing information for all Ge detectors that fired within 800 ns of the triggering signal. A total of 8.1×10^8 threefold and higher events were recorded. The beam, coming in bursts with ~ 0.3 ns time width, was pulsed with an ~ 400 ns repetition time, providing clean separation of prompt and isomeric events, which simplified the observation of γ - γ correlations across isomers. Conditions set on the γ - γ time parameter were used to obtain various versions of prompt-prompt and prompt-delayed γ - γ coincidence matrices as well as prompt γ - γ - γ and prompt γ - γ -delayed γ cubes covering γ -ray energy ranges to ~ 4 MeV.

The 11^- state, arising from the aligned $\pi h_{9/2} \nu i_{13/2}^{-1}$ coupling, located at 858 ± 3 keV above the 10^- millisecond isomer, should decay by an $M1$ transition to the isomeric state. As a first step towards identifying γ -ray cascades feeding the 10^- isomer, a search was made aimed at finding the $11^- \rightarrow 10^-$ ^{208}Bi γ ray in cross coincidence with known γ rays in reaction partner $A=44-47$ potassium nuclei. Coincidence spectra, double gated on pairs of γ rays in each of these K isotopes, examples of which are presented in Figs. 1(a) and 1(b), indeed showed an intense 855.7-keV Bi γ ray that could be confidently identified as the sought for ^{208}Bi transition. Many other γ rays could also be assigned to ^{208}Bi by

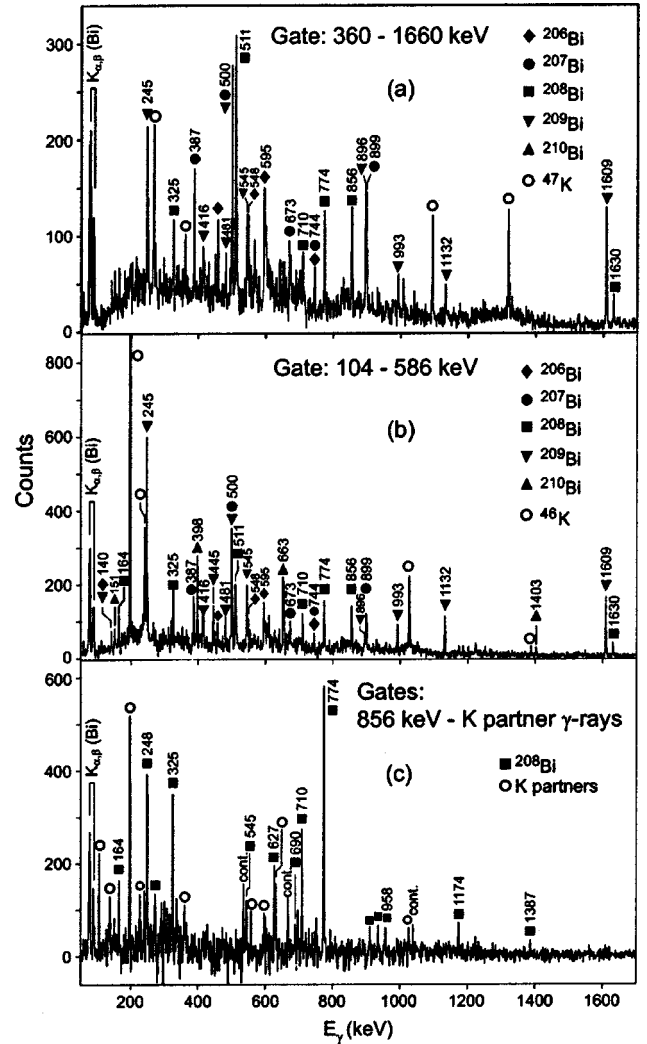


FIG. 1. Representative γ -ray coincidence spectra for potassium nuclei that are reaction partners to ^{208}Bi . (a,b) show γ rays coincident with double gates on the ^{47}K and ^{46}K transitions specified. (c) displays γ rays coincident with the 856-keV ^{208}Bi transition and the strongest transitions from the complementary $A=44-47$ K products.

setting double gates on the 856-keV γ ray and on known transitions in K isotopes; the identification in this way of the intense cascade of 774, 248, 710, and 325-keV γ rays with a 958-keV crossover is illustrated in Fig. 1(c).

Further inspection of the double gates set on these newly found transitions, examples of which are displayed in Fig. 2, revealed a weaker 151-keV γ ray belonging to the cascade and other crossovers of 1630, 1035, 476, and 1186 keV. As a result, levels were located at 3201, 3449, 4159, 4484, and 4635 keV. Another significant finding is a 2588-keV γ ray deexciting the level at 4159 keV and populating directly the 10^- isomer. Intensity balance of the 248, 774, 856, and 1630-keV γ rays, obtained by gating on γ rays cascading into the 3449-keV level, was used to extract the conversion coefficient $\alpha_{\text{tot}} = 0.8(2)$ for the 248-keV transition, showing that it is of $M1$ character.

Coincident spectra obtained by gating on the 856-keV γ

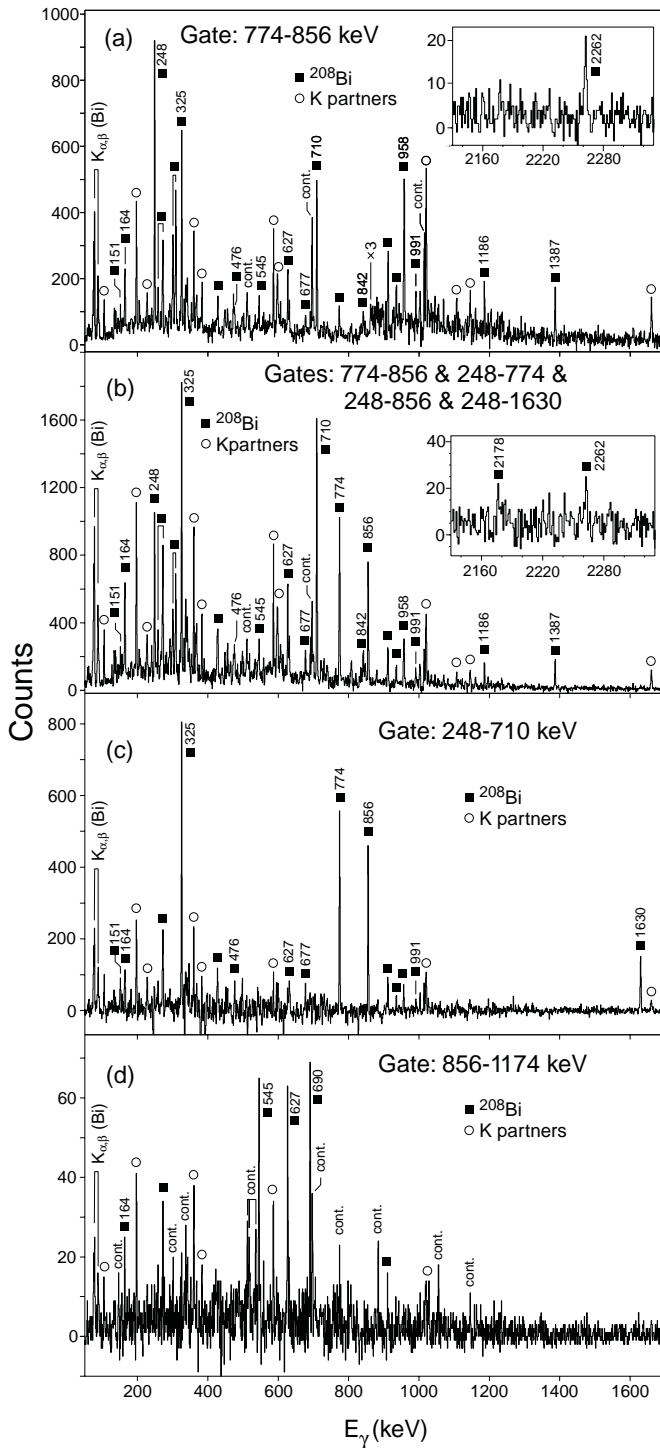


FIG. 2. Representative γ -ray coincidence spectra for ^{208}Bi . (a), (b), and (d) show γ rays coincident with double gates on the ^{208}Bi transitions specified. Contaminant lines of known origin are also indicated.

ray and on the transitions from the reaction partner nuclei showed also a second cascade of γ rays with energies 1174, 690, 545, 627, and 164 keV. All these γ rays were found to be in mutual coincidence [see Fig. 2(d) for the spectrum double gated on 856- and 1174-keV transitions], but the ordering was a problem. Observation of 842, 1387, 677, and

2262-keV γ rays, connecting this new level structure with the established levels, clarified the situation and levels at 3601, 4291, 4836, and 5463 keV were firmly located. The high intensity of the 164-keV γ ray suggested that it feeds the level at 5463 keV from a state at 5627 keV. The finding of 991-keV and 2178-keV transitions, deexciting the 5627-keV level into the levels at 4635 keV and 3449 keV, confirmed that location.

Data analysis also showed a number of other γ transitions, which could be firmly identified as high-lying γ rays in ^{208}Bi , but they could not be placed in the level scheme. In particular, a cascade of prompt 272, 456, 773, 912, 1015-keV lines was observed above the 5627-keV state. This cascade, as well as the γ rays located in the level scheme, were subsequently found to be delayed with respect to the group of transitions with energies 321, 557, 591, 607, and 1160 keV, which indicated a presence of an isomer at about 9.0 MeV. Following analysis of the $T_{\gamma-\gamma}$ spectrum for the two mentioned groups of γ rays yielded an estimate of ≈ 40 ns for the half-life of this isomer.

All γ -ray transitions identified in ^{208}Bi in this work are listed in Table I, and the final ^{208}Bi level scheme is presented in Fig. 3. This level scheme includes a state at 3500 keV deexciting by a 1929-keV γ ray, which will be discussed in the following section.

III. DISCUSSION

A. Overlap with charged particle spectroscopy studies

We have already described how the $^{209}\text{Bi}(p,d)$ transfer reaction results [1] helped us to recognize the 855.7-keV γ ray as the $11^- \rightarrow 10^-$ transition between $\pi h_{9/2} \nu i_{13/2}^{-1}$ states in ^{208}Bi . Next should come the highest spin states of $1p-1h$ character, those belonging to the $\pi i_{13/2} \nu i_{13/2}^{-1/2}$ multiplet. The two strongly populated levels located at 3201 and 3449 keV (Fig. 3) appear very good candidates to be the highest spin, 12^+ and 13^+ , members of that multiplet. The 3449-keV level is probably identical with a state observed at about 3.4 MeV in a $^{208}\text{Pb}(p,n)$ charge exchange reaction study [3], where it was tentatively interpreted as the maximally aligned ($\pi i_{13/2} \nu i_{13/2}^{-1/2}$) 13^+ state. The present results support that identification and determine the excitation energy more accurately. The 248-keV transition between the 3449 and 3201-keV levels has been shown to have $M1$ character from its total conversion; this means, that the connected states have the same parity and it is consistent with 13^+ and 12^+ assignments.

The present γ -ray results also overlap with those from $^{206}\text{Pb}(\alpha,d)$ transfer [4,5], which located several two-particle, two-hole states in ^{208}Bi . From their energies and their decay properties (which will be discussed later), it appears almost certain that the states at 3601 and 4836 keV (Fig. 3) are identical with the 12^+ and 14^- states of $\pi h_{9/2} \nu j_{15/2}(\nu^{-2})_0$ and $\pi i_{13/2} \nu j_{15/2}(\nu^{-2})_0$ character, located at 3609(7) and 4848(10) keV, respectively, in the (α,d) study. Another excitation of this type, the 11^+ state of $\pi i_{13/2} \nu g_{9/2}(\nu^{-2})_0$ character at 3508(7) keV, was also identified in (α,d) . The γ -ray decay of such an 11^+ state would

TABLE I. List of γ rays identified in ^{208}Bi , including intensities and placements. γ transitions that could not be placed in the level scheme are listed with their intensities in the bottom part of the table.

| γ -Ray energy E_γ (keV) | Intensity I_γ | Initial level energy E_i (keV) |
|--|-------------------------|-------------------------------------|
| 151.0(5) | 5 | 4635.3(10) |
| 163.7(5) | 11 | 5626.7(10) |
| 248.4(3) | 42 | 3449.4(7) |
| 325.2(3) | 28 | 4484.3(9) |
| 475.9(6) | 5 | 4635.3(10) |
| 545.2(4) | 13 | 4836.2(8) |
| 558.8(8) | 1 | 4159.1(8) |
| 626.8(4) | 15 | 5463.0(9) |
| 677.2(4) | 5 | 4836.2(8) |
| 690.3(4) | 7 | 4291.0(7) |
| 709.7(3) | 37 | 4159.1(8) |
| 774.4(3) | 79 | 3201.2(6) |
| 841.7(4) | 10 | 4291.0(7) |
| 855.7(2) | 100 | 2426.8(5) |
| 957.8(5) | 13 | 4159.1(8) |
| 990.8(7) | 4 | 5626.7(10) |
| 1034.9(5) | 4 | 4484.3(9) |
| 1173.9(4) | 15 | 3600.7(6) |
| 1185.9(4) | 5 | 4635.3(10) |
| 1336(1) | <1 | 4836.2(8) |
| 1386.7(4) | 8 | 4836.2(8) |
| 1629.9(3) | 45 | 3201.2(6) |
| 1928.6(10) | 3 | 3500(1) |
| 2178(1) | 1 | 5626.7(10) |
| 2262.0(8) | 3 | 5463.0(9) |
| 2588(1) | 2 | 4159.1(8) |
| 222.2(5) | 3 | |
| 257.8(5) | 5 | |
| 271.4(6) | 6 | |
| 272.3(5) | 11 | |
| 321.1(6) | 8 | |
| 337.2(8) | 9 | |
| 368.0(7) | 5 | |
| 426.3(7) | 6 | |
| 456.6(7) | 4 | |
| 557.2(6) | 5 | |
| 591.1(6) | 4 | |
| 607.2(6) | 5 | |
| 772.7(6) | 3 | |
| 911.6(4) | 8 | |
| 935.5(4) | 5 | |
| 956.8(6) | 5 | |
| 1002.4(5) | 4 | |
| 1015.0(7) | 9 | |
| 1159.8(4) | 5 | |
| 1196.8(7) | 2 | |

mainly feed the 10^- isomer directly, and a special search through all the coincidence spectra double gated on γ rays in the potassium partners revealed a 1929-keV γ ray as the likely $11^+ \rightarrow 10^-$ transition in ^{208}Bi ; it was placed feeding the 10^- isomer from a level at 3500 keV. Later analyses showed coincidence relationships between the 1929-keV γ ray and the higher-lying 690, 545, 627, 164-keV γ -ray cascade feeding the 3601-keV 12^+ state. This would imply a connecting 101-keV transition that should be of $M1$ character. Such a transition would have the total conversion coefficient of ~ 10 , making the 101-keV γ ray too weak to be detected in this experiment.

Finally, in support of the contention that the same $2p-2h$ states in ^{208}Bi have been seen both in (α, d) transfer and in the present γ -ray study, we note that the 11^+ , 12^+ , and 14^- level energies from (α, d) are systematically +8, +8, and +12 keV higher than the more accurate values determined here.

B. Shell model calculations

Our further efforts to interpret the high-spin levels of ^{208}Bi were heavily influenced by the results of shell model calculations described in this section. These calculations, in a space extending from ^{132}Sn to $^{310}\text{X}_{184}$ and including five proton-hole, six neutron-hole, six proton-particle, and seven neutron-particle orbitals with respect to the ^{208}Pb core have been performed with the OXBASH code [7]. The single-particle energies were taken from experiment as summarized in Ref. [8].

The basis for the residual interaction was the realistic interaction calculated by Kuo and Herling, using the Kuo-Brown method, from the measured interaction between free nucleons [9]. We have used it, but with the modifications applied in Refs. [10–12] to better fit experimental energies. This covered the interactions between particles, meaning orbitals above the shell gap, and those between holes, meaning orbitals below the gap. But for the particle-hole nucleus ^{208}Bi , the interaction between orbitals above and below the gap is of primary importance. This interaction has been recently calculated [13], again following the Kuo-Brown method [14], from the H7B interaction [15]. For the present calculations, we have checked and adjusted it to known one-particle one-hole states in ^{208}Bi . As a result, all diagonal proton neutron-hole elements have been shifted by -60 keV. In addition, the most important high-spin elements have been individually adjusted, namely, for the 10^- and 11^- states of the $\pi h_{9/2} \nu i_{13/2}^{-1}$ configuration by -82 and $+287$ keV and for the $(\pi i_{13/2} \nu i_{13/2}^{-1}) 13^+$ element by $+156$ keV. The results of the calculations for ^{208}Bi , including only yrast and near-yrast states in the spin range $I=10-17$, are shown in Table II.

The calculated energies of the one-particle, one-hole 10^- , 11^- , and 13^+ excitations agree well with experiment, as one might expect, since in each case the main matrix element was adjusted once to fit the experimental value. (Further iterations to achieve perfect agreement seemed pointless.) The energy of the 3201-keV 12^+ level is also well reproduced.

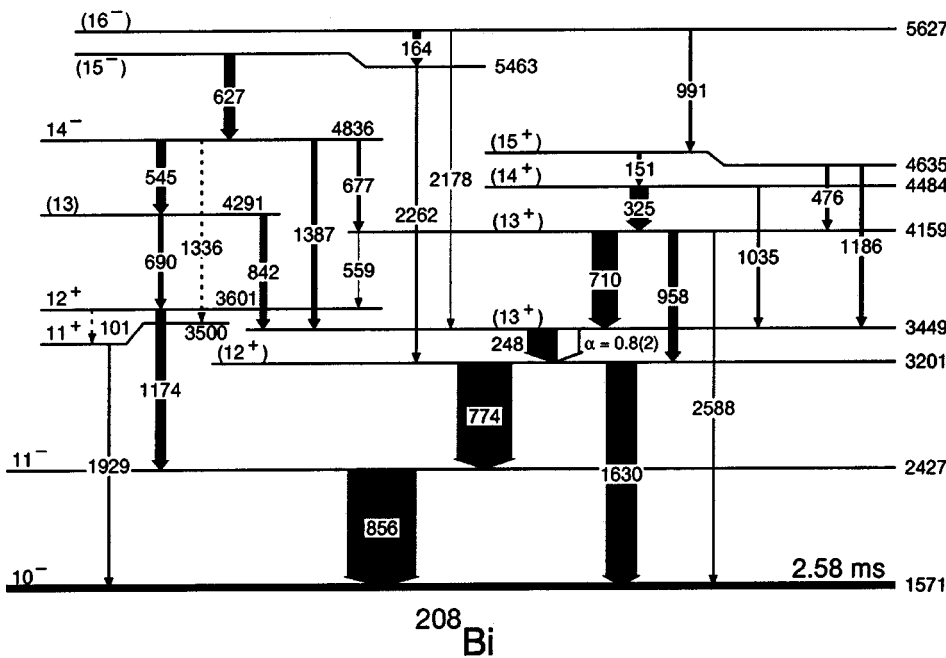


FIG. 3. The proposed level scheme for ^{208}Bi . Arrow widths denote the relative transition intensities.

Next we turn our attention to the 11^+ , 12^+ , and 14^- $2p$ - $2h$ states that were also seen in the $^{206}\text{Pb}(\alpha, d)$ reaction. As can be seen in Table II, the calculated and experimental energies agree very well. In the nuclei of the ^{208}Pb region, the fast $E3$ transition from $\nu j_{15/2}$ to $\nu g_{9/2}$ has often been found to compete with lower multipolarity transitions [16]. The 14^- and 11^+ states under discussion differ in just this orbital, and a weak 1336-keV transition between them is indeed seen. It is worth noting that the $(\pi i_{13/2} \nu j_{15/2} \nu_0^{-2}) 14^-$ level is not an yrast state in the calculations. Another 14^- state with the main component $\pi h_{9/2} \nu i_{11/2} (\nu^{-2})_4$ is calculated 18 keV lower, but such a state cannot be populated in $^{206}\text{Pb}(\alpha, d)$, and the γ -ray branch to the 11^+ level would be most unlikely. Since the γ -ray data fully support the assignments from charged particle reaction spectroscopy, the spin-parity assignments for the levels discussed so far may be regarded as certain. The selection rules for γ -ray decay then limit the possible spin assignments for the higher-lying levels. The good agreement of the shell model calculations in these clearcut cases also bolsters confidence in further configuration assignments for higher-lying states, based on comparing calculated energies with experiment.

Above the assigned 13^+ yrast state at 3449 keV, the calculations predict two other 13^+ excitations, at 4278 and 4340 keV, arising from more complicated configurations. The second state has a very fragmented structure, which resembles the composition of the 3^- octupole excitation in ^{208}Pb (arising from many $1p$ - $1h$ excitations) with $h_{9/2}$ proton and $i_{13/2}$ neutron hole added to each component. We interpret the level calculated at 4340 keV as a state of $(\pi h_{9/2} \nu i_{13/2}^{-1}) 10^- \times 3^-$ type, and assign it to the experimental level at 4159 keV, as will be further discussed in the framework of particle-octupole coupling.

The other 13^+ state, calculated at 4278 keV with the main component $\pi h_{9/2} \nu j_{15/2} p_{1/2}^{-1} f_{5/2}^{-1}$, might correspond to the level located at 4291 keV. The energy is very close (within

13 keV), and the γ -decay pattern is compatible with the theoretical configuration. The γ decay from and into the 4291-keV level sets strict limits on its spin. For the observed γ -ray energies, the $M2$ and $E3$ multiplicities cannot compete with the $E1$, $M1$, and $E2$ transitions, even if these are weak. Then, the only possible assignments are: 12^- , 13^- , 13^+ , and 14^+ . The 12^- is unlikely because of the absence of a transition to the 11^- . In turn, the two 13^- levels are calculated at 4357 and 4380 keV, and the 13^- assignment cannot be ruled out. The 14^+ possibility is much less probable as the 14^+ excitations are calculated at 4479 and 4554 keV, too far away when comparing with much better agreement achieved for the other states.

The calculations predict the 14^+ and 15^+ yrast states at 4479 and 4635 keV, respectively, both with the main configuration $\pi h_{9/2} \nu g_{9/2} i_{13/2}^{-1} p_{1/2}^{-1}$ (66% and 75%). It is very likely that the excitations located at 4484 and 4635 keV correspond to these 14^+ and 15^+ states. The state at 4484 keV decays by a strong 325-keV γ ray to the 13_2^+ excitation and by a weak 1035-keV branch to the 13_1^+ state, which is consistent with the proposed $J^\pi = 14^+$ assignment. The 4635-keV level decays by 151, 476 and 1186-keV transitions to the 14^+ , 13_2^+ , and 13_1^+ states, respectively. The 151-keV branch is the strongest, which is in accord with the same nature of the 15^+ and 14^+ states.

The shell model calculations give the first three $J^\pi = 15^-$ states at 5481, 5591, and 5650 keV, with the main configurations $\pi i_{13/2} \nu j_{15/2} p_{1/2}^{-1} f_{5/2}^{-1}$, $\pi i_{13/2} \nu g_{9/2} p_{1/2}^{-1} i_{13/2}^{-1}$, and $(\pi i_{13/2} \nu i_{13/2}^{-1}) 12^+ \times 3^-$, respectively. We tentatively associate a level at 5463 keV with one of these states. The connection to the 14^- state by a 627-keV γ ray is in line with a $J^\pi = 15^-$ assignment. Because a 2262-keV transition is observed to the 12^+ level, this state is probably the octupole excitation on top of the $(\pi i_{13/2} \nu i_{13/2}^{-1}) 12^+$ level, to be discussed below.

TABLE II. Yrast and near-yrast states up to spin $J = 17$ in ^{208}Bi . Spin-parity values, main configurations, and calculated energies are given in the first three columns, energies of the associated experimental levels in the fourth column and, references to the previous works for the relevant levels in the fifth column.

| J^π | Main configuration | Calculated energy (keV) | Experimental energy (keV) | Previous works |
|----------|---|-------------------------|---------------------------|----------------------|
| 10_1^- | $\pi h_{9/2} \nu i_{13/2}^{-1}$ | 1592 | 1571 | (<i>p,d</i>) [1] |
| 11_1^- | $\pi h_{9/2} \nu i_{13/2}^{-1}$ | 2449 | 2427 | (<i>p,d</i>) [1] |
| 12_1^+ | $\pi i_{13/2} \nu i_{13/2}^{-1}$ | 3242 | 3201 | |
| 13_1^+ | $\pi i_{13/2} \nu i_{13/2}^{-1}$ | 3420 | 3449 | (<i>p,n</i>) [3] |
| 11_1^+ | $(\pi i_{13/2} \nu g_{9/2}) \times \nu_0^{-2}$ | 3477 | 3500 | (α,d) [4,5] |
| 12_2^+ | $(\pi h_{9/2} \nu j_{15/2}) \times \nu_0^{-2}$ | 3640 | 3601 | (α,d) [4,5] |
| 13_2^+ | $\pi h_{9/2} \nu j_{15/2} p_{1/2}^{-1} f_{5/2}^{-1}$ | 4278 | 4291 | |
| 13_3^+ | $(\pi h_{9/2} \nu i_{13/2}^{-1}) \times 3^-$ | 4340 | 4159 | |
| 13_1^- | $\pi h_{9/2} \nu g_{9/2} f_{5/2}^{-2}$ | 4357 | | |
| 13_2^- | $\pi h_{9/2} \nu i_{11/2} p_{1/2}^{-1} f_{5/2}^{-1}$ | 4380 | | |
| 14_1^+ | $\pi h_{9/2} \nu g_{9/2} i_{13/2}^{-1} p_{1/2}^{-1}$ | 4479 | 4484 | |
| 14_2^+ | $\pi h_{9/2} \nu j_{15/2} p_{1/2}^{-1} f_{5/2}^{-1}$ | 4554 | | |
| 15_1^+ | $\pi h_{9/2} \nu g_{9/2} i_{13/2}^{-1} p_{1/2}^{-1}$ | 4635 | 4635 | |
| 14_3^+ | $\pi h_{9/2} \nu j_{15/2} p_{1/2}^{-1} f_{5/2}^{-1}$ | 4747 | | |
| 14_1^- | $\pi h_{9/2} \nu i_{11/2} f_{5/2}^{-2}$ | 4810 | | |
| 14_2^- | $(\pi i_{13/2} \nu j_{15/2}) \times \nu_0^{-2}$ | 4828 | 4836 | (α,d) [4,5] |
| 15_2^+ | $\pi h_{9/2} \nu j_{15/2} p_{1/2}^{-1} f_{5/2}^{-1}$ | 4879 | | |
| 15_3^+ | $\pi h_{9/2} \nu g_{9/2} f_{5/2}^{-1} i_{13/2}^{-1}$ | 4987 | | |
| 16_1^+ | $\pi h_{9/2} \nu g_{9/2} f_{5/2}^{-1} i_{13/2}^{-1}$ | 5076 | | |
| 16_2^+ | $\pi h_{9/2} \nu i_{11/2} p_{1/2}^{-1} i_{13/2}^{-1}$ | 5273 | | |
| 17_1^+ | $\pi h_{9/2} \nu g_{9/2} f_{5/2}^{-1} i_{13/2}^{-1}$ | 5338 | | |
| 15_1^- | $\pi i_{13/2} \nu j_{15/2} p_{1/2}^{-1} f_{5/2}^{-1}$ | 5481 | | |
| 17_2^+ | $\pi h_{9/2} \nu i_{11/2} f_{5/2}^{-1} i_{13/2}^{-1}$ | 5561 | | |
| 15_2^- | $\pi i_{13/2} \nu g_{9/2} p_{1/2}^{-1} i_{13/2}^{-1}$ | 5591 | | |
| 16_1^- | $\pi i_{13/2} \nu g_{9/2} i_{13/2}^{-1} p_{1/2}^{-1}$ | 5631 | | |
| 15_3^- | $(\pi i_{13/2} \nu i_{13/2}^{-1}) \times 3^-$ | 5650 | 5463 | |
| 17_1^- | $\pi i_{13/2} \nu g_{9/2} p_{1/2}^{-1} i_{13/2}^{-1}$ | 5741 | | |
| 16_4^- | $(\pi i_{13/2} \nu i_{13/2}^{-1}) \times 3^-$ | 5856 | 5627 | |

The highest-lying level in our level scheme is located at 5627 keV. It deexcites by a strong 164-keV γ ray and a weak 991-keV transition to the 15^- and 15^+ states, respectively, and again a high-energy 2178-keV transition to the $(\pi i_{13/2} \nu i_{13/2}^{-1}) 13^+$ state has been observed. This level might correspond to the very close lying, calculated 16^- state at 5631 keV with the main (77%) configuration of $\pi i_{13/2} \nu g_{9/2} i_{13/2}^{-1} p_{1/2}^{-1}$ type, but there are also other 15^- and 16^+ states calculated nearby. We, however, also in this case interpret the 2178-keV line as a stretched $E3$ transition, and consequently, the level as an octupole excitation built on the 13^+ state.

The fourth calculated 16^- level at 5856 keV shows a structure resembling this octupole excitation. It is a common feature, that the shell model calculations place the octupole levels about 200 keV too high in excitation energy. Here it is 181 keV for the 13^+ , 187 keV for 15^- , and 229 keV for 16^- . In ^{208}Pb , a similar difference of 205 keV is observed for the 17^+ state, the octupole excitation built on the $(\nu j_{15/2} \nu i_{13/2}^{-1}) 14^-$ state [13].

It is not clear why the calculated 17^+ and 16^+ yrast levels are not observed, but the two effects may contribute to it: first, the level population falls off sharply above the 14^+ state, and second, their decay involve highly converted $M1$ transitions.

C. Octupole excitations

The level at 4159-keV decays to the 13^+ , 12_1^+ , 12_2^+ , and 10^- states by 710, 958, 559, and 2588-keV γ rays, respectively. The 2588-keV branch to the 10^- isomer suggests that the 4159-keV level might correspond to the 13^+ state arising from the 3^- octupole excitation of the ^{208}Pb core (with 2615-keV ^{208}Pb unperturbed energy) built on the 10^- isomer. In such a case, the two transitions at 710 and 958 keV, connecting the 4159-keV 13_2^+ state with the 12^+ and 13^+ excitations at 3201 and 3449 keV of rather pure $\pi i_{13/2} \nu i_{13/2}^{-1}$ character, would be mediated by the admixture of the $\pi i_{13/2} \nu i_{13/2}^{-1}$ type in that 4159-keV 13_2^+ state. Under this assumption, the branching ratio $I(958)/I(710)=0.3$ is given simply by the geometrical factor that accounts for the differ-

ent spins 12^+ and 13^+ of the final states. It agrees very well with the experimental value of 0.35(6). The summed $M1$ rate for the 710 and 958-keV transitions can be calculated from the known g factors of the $i_{13/2}$ proton particle and the $i_{13/2}$ neutron hole as $(2.6 \times 10^{13} \text{ s}^{-1}) \times \text{admixture}$. Taking for the $B(E3; 13^+ \rightarrow 10^-)$ a value of 30–40 W.u., one gets the rate $(3.0\text{--}4.5) \times 10^{10} \text{ s}^{-1}$ for the 2588-keV transition. The experimental branching ratio is $I(710+958)/I(2588) = 24(6)$, which implies an admixture of the order of 4%.

The energy of the 3^- octupole state built on the $(\pi h_{9/2} \nu i_{13/2}^{-1}) 10^-$ isomer can be estimated taking into account the individual energy shifts of the octupole excitations built on the $\pi h_{9/2}$ and $\nu i_{13/2}^{-1}$ orbitals as $2615 + 126 - 130 = 2611 \text{ keV}$, close to the experimental energy of 2588 keV. One has to note that such a simple summation of the energy shifts would be appropriate only for the octupole built on the stretched $(\pi h_{9/2} \nu i_{13/2}^{-1}) 11^-$ state. Since, in the case we are considering now, the octupole is built on the 10^- state, which is a $J_{\text{max}}-1$ excitation, the shift should be slightly changed. However, the main feature that the expected shift should be small, remains unaltered.

The 12^+ 3201-keV state is of $\pi i_{13/2} \nu i_{13/2}^{-1}$ type. The energy of the 2262-keV line from the 15^- level is shifted by -353 keV from the 2615-keV pure octupole energy in ^{208}Pb . One expects the shift to be the sum of that of the individual orbitals times a geometrical factor $10/13$, because the coupling is not stretched [17]. The shift is directly known as $2485 - 2615 = -130 \text{ keV}$ for the $\nu i_{13/2}^{-1}$ configuration in ^{207}Pb . For the $\pi i_{13/2}$ orbital in ^{209}Bi , it has to be calculated. The octupole coupling constant might be taken between $h = 730 \text{ keV}$ as found for the $i_{13/2}$ neutron hole [17] and $h = 930 \text{ keV}$ [18]. The theoretical value $h = 910 \text{ keV}$ [19] is also close. The shift is then -248 keV and -282 keV , respectively. This is about twice the shift for the $i_{13/2}$ neutron hole, because the $i_{13/2}$ proton is above its partner $f_{7/2}$, while the sequence is reversed for the neutron holes. In total, this gives the expected shift for ^{208}Bi $(-130 - 260)/1.3 = -300 \text{ keV}$ close to the measured value of -353 keV .

The $B(E3, 15^- \rightarrow 12^+)$ likely exceeds 50 W.u. This has been found for similar cases [20], if two strongly octupole coupled orbitals contribute. The decay rate is then $\lambda(E3) \geq 2.3 \times 10^{10} \text{ s}^{-1}$. The $M1$ branch with 627 keV to the 14^- level is experimentally five times stronger, or $\lambda(M1) \geq 1.1 \times 10^{11} \text{ s}^{-1}$, corresponding to 0.015 W.u. That can well be possible as the structure of the two states is different. In the same way, the level at 5627 keV might be regarded as 16^- , the octupole excitation of the stretched $(\pi i_{13/2} \nu i_{13/2}^{-1}) 13^+$ state, as they are connected by a 2178-keV line. The expected energy is $2615 - 390 = 2225 \text{ keV}$. In conclusion, three levels can be well explained as octupole excitations built on one-particle, one-hole levels.

D. Comparison with ^{132}Sb

There is a general close resemblance between the spectroscopy of the ^{132}Sn and the ^{208}Pb regions. The orbitals above and below the energy gaps in the two cases are similarly ordered, and every single-particle state in the ^{132}Sn re-

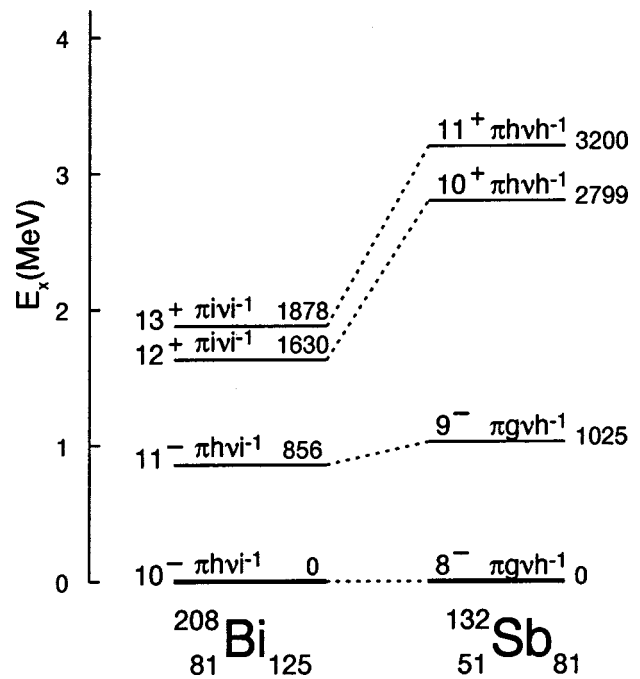


FIG. 4. Comparison of yrast one-particle, one-hole states in ^{208}Bi and ^{132}Sb . Dominant shell model configurations are indicated.

gion has its counterpart around ^{208}Pb with the same radial quantum number n and one unit larger in angular momenta l and j . Only recently a few yrast states were located in the $\pi \nu^{-1}$ ^{132}Sb nucleus [21], which is the counterpart of $\pi \nu^{-1}$ ^{208}Bi . The 10^- and 11^- states in ^{208}Bi of $\pi h_{9/2} \nu i_{13/2}^{-1}$ character correspond to the 8^- and 9^- excitations in ^{132}Sb arising from the $\pi g_{7/2} \nu h_{11/2}^{-1}$ configuration. Similarly, the 12^+ and 13^+ states in ^{208}Bi of the $\pi i_{13/2} \nu i_{13/2}^{-1}$ type have partners in the 10^+ and 11^+ members of the $\pi h_{11/2} \nu h_{11/2}^{-1}$ multiplet in ^{132}Sb (Fig. 4). In both cases the energy difference between the $j_{\text{max}}-1$ states of the corresponding configurations, i.e., between the 12^+ and 10^- excitations in ^{208}Bi and 10^+ and 8^- in ^{132}Sb are very close to the energy difference of the single-particle energies of the proton orbitals involved. In ^{208}Bi , the 12^+ and 10^- excitations are connected by a 1630-keV transition, which is the obvious counterpart of the 1609-keV $\pi i_{13/2} \rightarrow \pi h_{9/2}$ $M2$ transition in the neighboring one-proton nucleus ^{209}Bi . In ^{132}Sb , the corresponding 10^+ state decays to the 8^- excitation by a 2799-keV γ ray, which again is very close to the 2792 keV one of the $\pi h_{11/2} \rightarrow \pi g_{7/2}$ $M2$ transition in ^{133}Sb .

In recent works [21–23], specific nucleon-nucleon interactions needed for shell model calculations in nuclei around ^{132}Sn were estimated from empirical interactions known for corresponding ^{208}Pb region nuclei. Thus, from the 856-keV 10^- - 11^- spacing in the ^{208}Bi $\pi h_{9/2} \nu i_{13/2}^{-1}$ multiplet, one could estimate, using $A^{-1/3}$ scaling to take account of the size difference, that the 8^- - 9^- spacing for the $\pi g_{7/2} \nu h_{11/2}^{-1}$ multiplet in ^{132}Sb should be 996 keV, in good agreement with experiment. However, a similar comparison between the $\pi h_{11/2} \nu h_{11/2}^{-1}$ 10^+ - 11^+ spacing of 401 keV in ^{132}Sb and the $\pi i_{13/2} \nu i_{13/2}^{-1}$ 12^+ - 13^+ spacing of 248 keV in ^{208}Bi gives less

satisfactory agreement, possibly reflecting mixing of other configurations in the ^{208}Bi case.

IV. SUMMARY

Detailed γ -ray coincidence measurements using Gamma-sphere for the reaction system $^{208}\text{Pb} + 305 \text{ MeV } ^{48}\text{Ca}$ have provided much information about yrast and near-yrast excitations in ^{208}Bi above the known 10^- isomer. The new findings include high-spin members of $\pi\nu^{-1}$ multiplets and states arising from two-particle, two-hole couplings. Considerable overlap between the present data and those from earlier charged particle spectroscopy studies was important in the interpretation of the ^{208}Bi levels, as well as comparisons

with results of extensive shell model calculations. Among the $2p$ - $2h$ states, three levels were explained as octupole excitations built on specific $1p$ - $1h$ states, and their energies were shown to be consistent with empirical predictions. Where possible, the $1p$ - $1h$ states in ^{208}Bi are compared with corresponding excitations in its counterpart $\pi\nu^{-1} \text{ } ^{132}\text{Sb}$ nucleus.

ACKNOWLEDGMENTS

This work was supported by the U.S. Department of Energy under Contracts No. DE-FG02-87ER40346 and No. W-31-109-ENG-38, and by the Polish Scientific Committee Grant No. 2PO3B-074-18.

-
- [1] G.M. Crawley, E. Kashy, W. Lanford, and H.G. Blosser, Phys. Rev. C **8**, 2477 (1973).
 - [2] M.J. Martin, Nucl. Data Sheets **47**, 797 (1986).
 - [3] B.D. Anderson, C. Lebo, A.R. Baldwin, T. Chittrakarn, R. Madey, J.W. Watson, and C.C. Foster, Phys. Rev. Lett. **52**, 1872 (1984).
 - [4] W.W. Daehnick, M.J. Spisak, R.M. DelVecchio, and W. Oelert, Phys. Rev. C **15**, 594 (1977).
 - [5] M.J. Spisak, and W.W. Daehnick, Phys. Rev. C **29**, 2088 (1984).
 - [6] R. Broda, Eur. Phys. J. A **13**, 1 (2002), and references therein.
 - [7] B.A. Brown, A. Etchegoyen, W.D.M. Rae, N.S. Goldwin, W.A. Richter, C.H. Zimmerman, W.E. Ormand, and J.S. Winfield, MSU-NSCL Report No. 524, 1985.
 - [8] M. Rejmund, M. Schramm, and K.H. Maier, Phys. Rev. C **59**, 2520 (1999).
 - [9] T.T.S. Kuo and G.H. Herling, U.S. Naval Research Laboratory Report No. 2258, 1971 (unpublished).
 - [10] E.K. Warburton and B.A. Brown, Phys. Rev. C **43**, 602 (1991).
 - [11] L. Rydstrom, J. Blomqvist, R.J. Liotta, and C. Pomar, Nucl. Phys. **A512**, 217 (1990).
 - [12] J.B. McGrory and T.T.S. Kuo, Nucl. Phys. **A247**, 283 (1975).
 - [13] M. Rejmund, Ph.D. thesis, Institute of Experimental Physics, Warsaw University, 1998.
 - [14] T.T.S. Kuo and G.E. Brown, Nucl. Phys. **85**, 40 (1966).
 - [15] A. Hosaka, K.I. Kubo, and H. Toki, Nucl. Phys. **A444**, 76 (1985).
 - [16] J. Wrzesiński, K.H. Maier, R. Broda, B. Fornal, W. Królas, T. Pawlat, D. Bazzacco, S. Lunardi, C. Rossi Alvarez, G. de Angelis, A. Gadea, J. Gerl, and M. Rejmund, Eur. Phys. J. A **10**, 259 (2001).
 - [17] M. Rejmund *et al.*, Eur. Phys. J. A **8**, 161 (2000).
 - [18] A.P. Byrne, S. Bayer, G.D. Dracoulis, and T. Kibédi, Phys. Rev. Lett. **80**, 2077 (1998).
 - [19] I. Hamamoto, Phys. Rep. **10**, 63 (1974).
 - [20] S.J. Poletti, G.D. Dracoulis, A.R. Poletti, A.P. Byrne, and A.E. Stuchberry, Nucl. Phys. **A448**, 189 (1986).
 - [21] P. Bhattacharyya *et al.*, Phys. Rev. C **64**, 054312 (2001).
 - [22] C.T. Zhang *et al.*, Phys. Rev. Lett. **77**, 3743 (1996).
 - [23] P. Bhattacharyya *et al.*, Phys. Rev. Lett. **87**, 062502 (2001).